THE EFFECT OF POLARIZATION ON THE ELECTROCHEMICAL BEHAVIOR OF Ti-13Nb-13Zr ALLOY

S. L. Assis and I. Costa*
IPEN/CNEN-SP/ Materials Science and Technology Centre,
Av. Prof. Lineu Prestes 2242, São Paulo, SP, Brazil
Phone: +55 11 3816 9356 Fax: +55 11 3816 9370
E-mail icosta@ipen.br

ABSTRACT

The effect of potentiostatic polarization on the electrochemical behavior of the Ti-13Nb-13Zr alloy was investigated by electrochemical impedance spectroscopy and potentiodynamic polarization curves in Hanks' solution at 37 ^{o}C. The polarization curves indicated a passive behaviour; however the current increased slightly at potentials around 1300 mV. Based on the potentiodynamic polarization curves, the potentiostatic polarization potentials were chosen and EIS diagrams were sequentially obtained at the open circuit potential (OCP), 500 mV and 1300 mV. The experimental results were interpreted using equivalent electrical circuits The equivalent circuit representing the results at OCP and 500 mV were associated to a duplex structure oxide, composed of an inner barrier layer and a porous outer layer. Polarization at 500 mV caused the thickening of both layers, barrier and porous, however, the barrier layer, that is mainly accountable for the corrosion resistance, became increasingly more defective with polarization potential, leaving a highly defective oxide on the alloy surface polarized at 1300 mV. The results suggested that the current increase at potentials around 1300 mV could be related to the deterioration of the barrier layer on the Ti alloy.

Key words: Passive films, Ti-13Nb-13Zr, potentiodynamic polarization curves, electrochemical impedance spectroscopy, biomaterials

INTRODUCTION

Titanium alloys are very resistant to corrosion due to the highly protective oxide film, mainly composed of TiO_2 that covers the metallic substrate. This oxide film is spontaneously formed on the Ti alloy surface when exposed to the atmosphere. The thickness of the film is initially approximately 1.4 nm, but it reaches 5 nm after 70 days, 8 to 9 nm after 545 days and 25 nm after 4 years of atmospheric exposure[1]. When this film is damaged, resulting in the exposure of the metallic substrate, it is rapidly repaired if in the atmosphere there are traces (ppm) of oxygen or humidity. Due to their high corrosion resistance associated to high mechanical properties, such as high strength-to-weight ratio, these alloys find wide applications, among them, as biomaterials for implants fabrication. Their electrochemical behaviour and oxide properties characterization have been largely investigated and, in many of these studies, electrochemical methods have been used, such as electrochemical impedance spectroscopy and polarization methods. Cai *et al.*[2,3] investigated the electrochemical behaviour of titanium and titanium alloys with various surface finishing, in synthetic saliva, and the results showed an extensive passive region for these materials from the corrosion potential until approximately 1600 mV (vs. Ag/AgCl). A large increase in current density occurred for potentials higher than this last potential, and the authors related it to the oxide film breakdown. However, at higher potentials, a decrease in current density was indicated in the polarization curves. Kolman and Scully [4,5] studied the passivity behaviour of β-type titanium alloys and also observed an increase in current density at potentials of approximately 1600 mV (SCE), in chloride solution. Oppositely to Cai *et al.*, Kolman and Scully attributed the current increase to the oxygen evolution reaction. They used optical microscopy to investigate the alloy surface after polarization but pits were not found on it. According to the last authors, pitting does not occur on these alloys until polarization potentials of the order of 9 V. According to Kolman and Scully the decrease in current density at potentials of approximately 1900 mV (SCE) was due to the decrease in the rate of the oxygen evolution reaction caused by hindered charge transfer processes through the growing oxide film. This was also observed for other Ti alloys, at different potentials. Other researchers[6] also observed this current density increase around this potential, with even larger rates, when the polarization curves were obtained in more complex solutions, such as a MEM culture medium[7].

Therefore, there is no general agreement on the causes for the current increase at potentials in the range from 1300 to 1600 mV, followed by its decrease at higher potentials. The aim of this study was to evaluate the effect of potentiodynamic polarization on the electrochemical behaviour of the Ti-13Nb-13Zr alloy using polarization curves and electrochemical impedance spectroscopy (EIS), and also to investigate the causes of current density increase at potentials around 1300 mV.

MATERIALS AND METHODS

The near-β Ti-13Nb-13Zr alloy used in this study was laboratory prepared by Schneider[8], and their chemical composition, determined by inductively coupled plasma - atomic emission spectroscopy (ICP-AES), is shown in Table 1. This alloy was obtained by melting pure Ti and Nb (99.9%), and Zr containing up to 4.5% of Hf, in an arc melting furnace, using a non consumable electrode, in an argon atmosphere. After melting, the ingot was heat treated for 1 hour at 1000 ^{o}C, followed by water-cooling, for homogenization. Subsequently, the alloy was cold worked (forged) until a diameter of 6.5 mm. During the stage of forging the alloy was once again heat treated at 1000 ^{o}C, followed by water cooling[(8)].

Table 1. Chemical composition of Ti-13Nb-13Zr alloy.

Element	C	H	N	O	S	Hf	Fe	Nb	Zr	Ti
% (mass)	0.035	0.011	0.004	0.075	<0.001	0.055	0.085	13.18	13.49	Bal.

Electrodes were prepared by epoxy cold resin mounting of the alloy, leaving an area corresponding to 0.33 cm^2 for exposure to the electrolyte. The surface for exposure to the electrolyte was prepared by sequential grinding with silicon carbide paper up to #2000 finishing, followed by mechanical polishing with diamond paste of 1 μm. After polishing, the surface was degreased with acetone in an ultrasonic bath for 10 minutes and then, rinsed with deionized water. A three-electrode cell set-up was used for the electrochemical measurements, with a saturated calomel reference electrode (SCE) as reference electrode and a platinum wire as the auxiliary electrode. The electrolyte used to simulate the physiological medium was Hanks' solution, naturally aerated, whose composition is presented in Table 2. The pH of this

solution is 6.8, that is, very similar to that of the physiological fluids. After surface preparation and prior to EIS tests, all the samples remained immersed for 72 h in Hanks' solution, naturally aerated at 37 ^{o}C, and the open circuit potential was measured as a function of time, until a steady state was reached. A steady potential is necessary to validate the electrochemical impedance spectroscopy (EIS) results. The EIS diagrams were sequentially obtained, firstly at the open circuit potential (*OCP*) after 72 h of immersion, and then at 500 mV and 1300 mV. The EIS data at the various potentials were obtained with only one working electrode. After the EIS results have been obtained at *OCP* the electrode was potentiostatically polarized at 500 mV for 20 minutes and then another EIS test was performed at this potential. Next, the electrode was polarized at 1300 mV for 20 minutes and subsequnetly the EIS measurements were obtained. EIS tests were carried out by means of a Solartron SI-1255 frequency response analyser coupled to a EG&G PARC 273A potentiostat and controlled by a software (Zplot). EIS measurements were performed in potentiostatic mode and the frequency range studied was from 100 kHz to 10 mHz. The amplitude of EIS perturbation signal was 10 mV with a data acquisition rate of 6 points per decade. Polarization was carried out using an EG&G PARC 273A Potentiostat in the potential range from -800 mV(SCE) to 3000 mV(SCE) and the scan rate was 1mV/s. All tests were carried out in naturally aerated and quiescent Hanks' solution at 37 ^{o}C.

Table 2 - Chemical composition of Hanks' solution.

Component	Concentration (Mol/L)
NaCl	0.1369
KCl	0.0054
$MgSO_4.7H_2O$	0.0008
$CaCl_2.2H_2O$	0.0013
$Na_2HPO_4.2H_2O$	0.0003
KH_2PO_4	0.0004
$C_6H_{12}O_6H_2O$	0.0050
Red phenol 1%	0.0071
pH	6.8

RESULTS AND DISCUSSION

Figure 1 shows a polarization curve for the Ti-13Nb-13Zr after 72 h of immersion in Hanks' solution. The current density increased with the polarization potential from the corrosion potential (*OCP*) until approximately 500 mV (SCE). From this last potential until nearly 1300 mV the current was fairly constant and in the order of 10^{-6} A/cm^2, that is, typical of a passive behaviour. The current increase with potential from *OCP* to 500 mV might be due to the relatively high scan rate used and consequently the thickening of the oxide film being insufficient to compensate the high field effects of polarization overpotential. At 1300 mV the current density increased but at approximately 1700 mV the current density stabilized at nearly 14 μA/cm^2 until the test was terminated at 3 V.

The Bode diagrams corresponding to the EIS results obtained at *OCP*, 500 mV and 1300 mV are shown in Figure 2. The polarization potentials (500 mV and 1300 mV) at which the EIS data were obtained were chosen from the polarization curves.

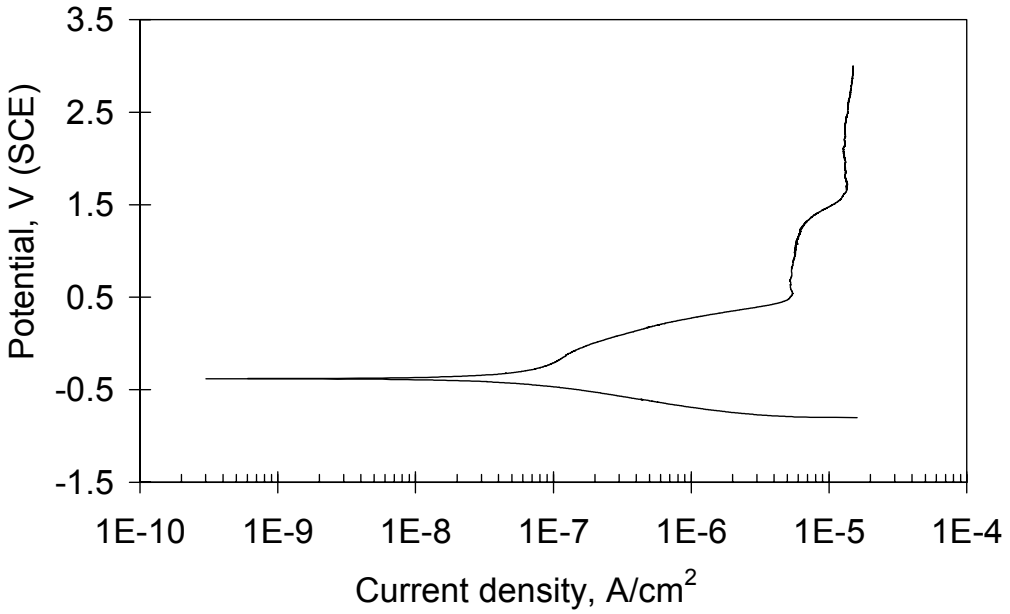

Figure 1 - Potentiodynamic polarization curve for Ti-13Nb-13Zr alloy after 72 h of immersion in Hanks' naturally aerated solution at pH 6.8 and 37 ^{o}C.

The EIS plots were interpreted using the Zview plot and the equivalent electrical circuits shown in Figure 3. The errors associated to each component proposed in the circuit were provided by the fitting.

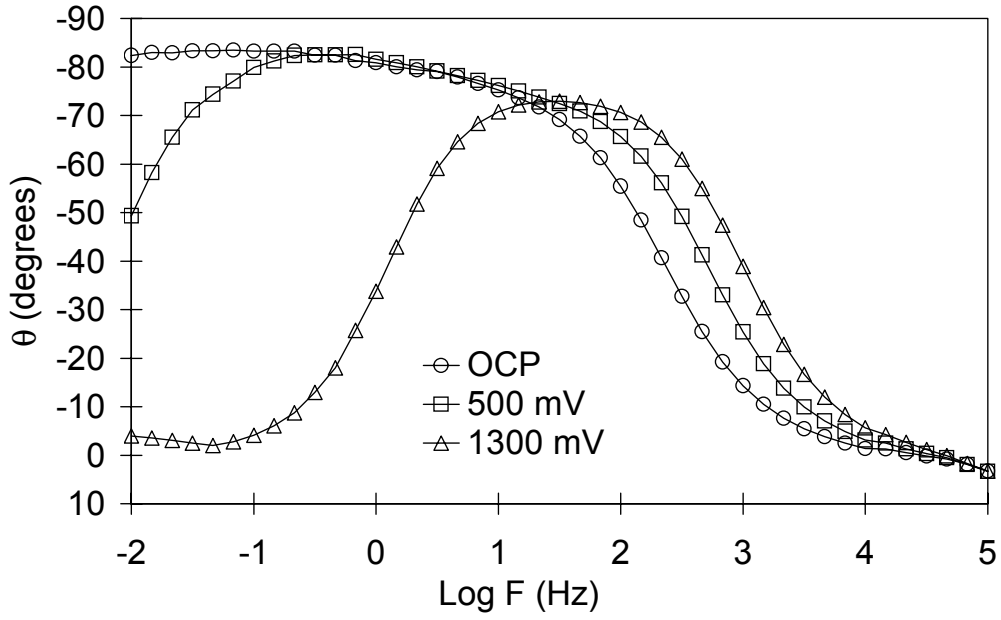

(a)

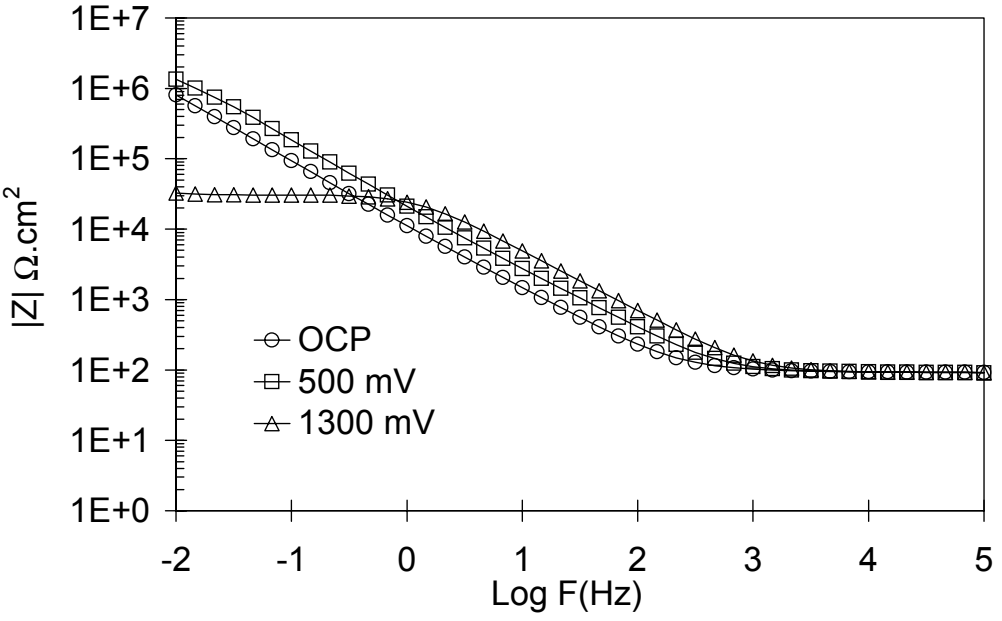

(b)

Figure 2 – Bode diagrams for Ti-13Nb-13Zr alloy after 72 h of immersion in Hanks' solution obtained at *OCP*, 500 mV and 1300 mV: (a) Phase angle Bode diagrams and (b) Z modulus Bode diagrams.

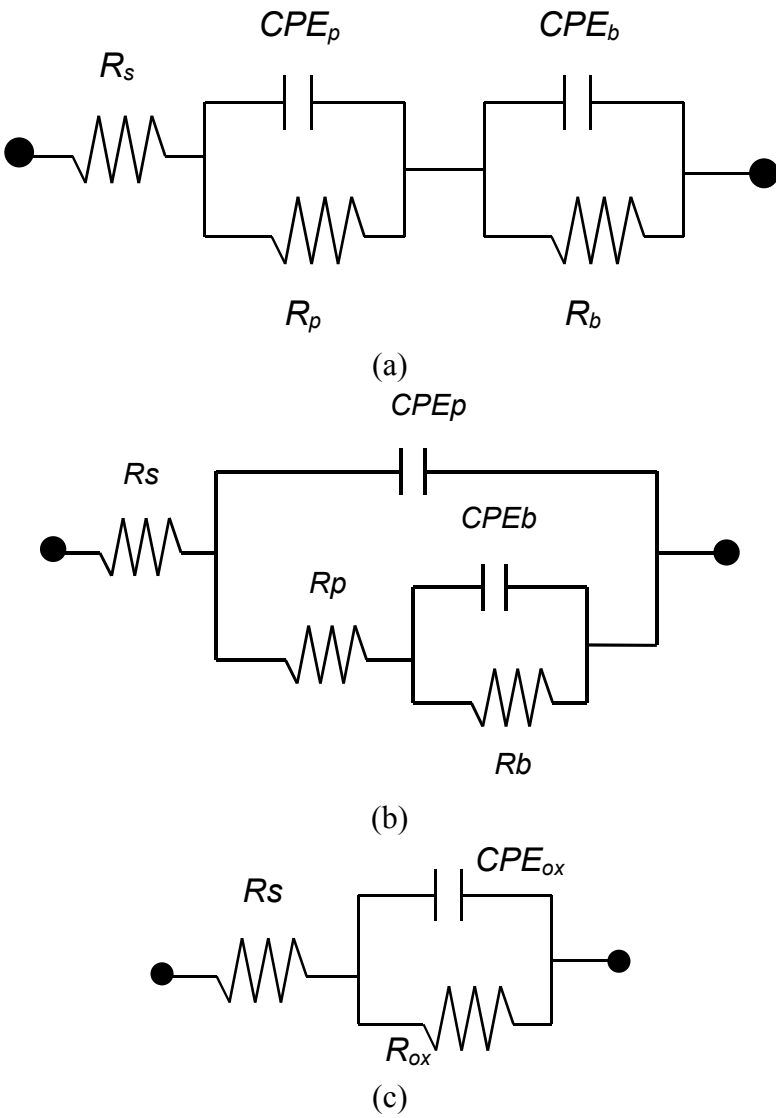

Figure 3 – Equivalent electrical circuits used for fitting experimental data obtained at (a) *OCP*, (b) 500 mV and (c) 1300 mV, which are shown in Figure 2.

The equivalent electrical circuit shown in Figure 3(a) was used by Kolman and Scully [4,5] and Yu *et al*.[9] to study oxide films on titanium and titanium alloys in aqueous environments, while that shown in Figure 3(b) was applied by Pan *et al.*[10] to investigate the electrochemical behaviour of titanium in phosphate buffer solution (PBS). These two circuits are based on the model of a duplex structure oxide composed of an inner barrier layer and an outer porous layer. This last layer contains microscopic pores whereas the barrier layer is compact and related to a very large resistance. The two circuits proposed contain resistance and constant phase elements. The components R_s, R_p and R_b are related to solution resistance, porous layer resistance and barrier layer, resistance, respectively. The constant phase elements, CPE_b e CPE_p are associated to the capacitive behaviour showed by the

barrier and porous layer, respectively. Incorporation of environment species into titanium alloys occur through the microscopic pores of the last layer. This might result in a slight increase in resistance with time. According to literature [11,12] this layer is associated to the biocompatibility presented by the titanium alloys. It is proposed that the time constant at intermediate frequencies is associated to this layer. Eventually, the pores might become sealed with the incorporated species from the medium.

The parallel components R_b and CPE_b, represent the processes occurring at the barrier layer and this layer has been associated to the high corrosion resistance of the titanium alloys. The CPE_b component is correlated to the capacitance of the barrier layer that is accountable for the high phase angles at low frequencies. On the other hand, R_b is related to the barrier layer resistance to mass and current transfer. The values of the electrical components obtained from fitting to the various equivalent electrical circuits proposed are shown in Table 3.

As the potential increased from *OCP* to 500 mV, the values of R_p increased and that of CPE_p decreased suggesting thickening of the porous layer. The higher phase angles obtained at 500 mV comparatively to *OCP* for the porous layer support the hypothesis of porous layer thickening. On the other hand, the barrier layer seems to have also been affected, with lower resistance values been obtained at 500 mV comparatively to *OCP*.

The equivalent electrical circuit shown in Figure 3(c), with only one time constant, fitted very properly the results obtained at 1300 mV. The results obtained at low frequencies and shown in the Bode phase angle diagram indicated a resistive behaviour, oppositely to that obtained at *OCP*. These results indicate deterioration of both layers, barrier and porous, as the potential polarization increased. According to literature[13], the change of the phase angle peak from medium frequencies to lower frequencies and the decrease in the capacitive behaviour are related to the deterioration of the oxide film properties.

Table 3. Values of electrical components obtained from fitting the circuits shown in Figure 3 to the experimental results from electrochemical impedance tests for 72 h immersion in Hanks' solution at 37 ºC of Ti-13Nb-13Zr alloy at three potentials.

Circuit element	Ti-13Nb-13Zr					
	OCP		500 mV		1300 mV	
	Circuit of Figure 3a		Circuit of Figure 3b		Circuit of Figure 3c	
	Value	**Error (%)**	**Value**	**Error (%)**	**Value**	**Error (%)**
R_s ($\Omega.cm^2$)	92.96	0.26	94.31	0.56	91.52	0.67
R_p ($K\Omega.cm^2$)	22.72	6.45	52.03	7.98	-	-
CPE_p ($\mu F.cm^{-2}$)	126.77	1.02	6.23	1.90	-	-
α_p	0.7337	#	0.9313	0.2690	-	-
$CPE_{b/ox}$ ($\mu F.cm^{-2}$)	16.78	0.30	2.00	5.50	4.70	1.20
$\alpha_{b/ox}$	0.9545	#	0.9441	#	0.8967	0.2249
$R_{b/ox}$ ($K\Omega.cm^2$)	898.93	9.58	234.18	3.25	31.71	0.70
χ^2	4.5E-4		1.7E-3		1.6E-3	

- Value was fixed.

It is proposed that the polarization at 500 mV promotes porous layer thickening and, at the same time, the introduction of defects in the barrier layer, partially exposing the metallic substrate. This is supported by the decrease in resistance and capacitance for the results obtained at 500 mV, comparatively to *OCP*, and even further, for the results at 1300 mV. For this last potential, the value of the "barrier" layer resistance was of the same order of that obtained for the porous layer at *OCP* suggesting that as the polarization potential increased the barrier layer became more defective, exposing the metallic substrate at the pores base. The relatively larger peak obtained at 1300 mV might include the contributions of both time constants, that related to charge transfer processes and that of the remaining porous oxide layer.

CONCLUSIONS

The results of this study indicated that polarization decreased the protective properties of the oxide film on the Ti-13Nb-13Zr alloy. For large overpotentials (1300 mV) the barrier layer becomes highly defective, exposing the metallic substrate at the base of defects and decreasing its resistance. The deterioration of the barrier layer might have caused the increase in current at potentials around 1300 mV, observed in the polarization curves.

REFERENCES

1. BIRCH, J.R.; BURLEIGH, T.D. Oxides formed on titanium by polishing, etching, anodizing, or thermal oxidizing. ***Corrosion***, v.56, n.12, p.1233-1241, 2000.

2. CAI, Z.; NAKAJIMA, H.; WOLDU, M.; BERGLUND, A.; BERGMAN, M.; OKABE, T. In vitro corrosion resistance of titanium made using different fabrication methods. ***Biomaterials***, v.20, p.183-190, 1999.

3. CAI, Z.; SHAFER, T.; WATANABE, I.; NUNN, M.E.; OKABE, T. Electrochemical characterization of cast titanium alloys. ***Biomaterials***, v.24, p.213-218, 2003.

4. Kolman, D.G.; Scully, J.R. Electrochemistry and passivity of Ti-15V-3Cr-3Al-3Sn β-titanium alloy in ambient temperature aqueous chloride solutions***. Journal of the Electrochemical Society***, v.141, n.10, p.2633-2641, 1994.

5. Kolman, D.G.; Scully, J.R. Electrochemistry and Passivity of a Ti-15Mo-3Nb-3Al beta-titanium alloy in ambient temperature aqueous chloride solutions***. Journal of the Electrochemical Society***, v.140, n.10, p.2771-2779, 1993.

6. Choubey, A.; Balasubramaniam, R.; Basau, B. Effect of replacement of V by Nb and Fe on the electrochemical and corrosion behavior of Ti-6Al-4V in simulated physiological environment. ***Journal of Alloys and Compounds***, v.381, p.288-294, 2004.

7. Assis, S.L. ***Investigação da resistência à corrosão da liga Ti-13Nb-13Zr por meio de técnicas eletroquímicas e de análise de superfície.*** 2006, 181p. Tese (Doutorado em Tecnologia Nuclear – Materiais) – Instituto de Pesquisas Energéticas e Nucleares, IPEN/CNEN-SP, São Paulo.

8. Schneider, S.G. ***Obtenção e caracterização da liga Ti-13Nb-13Zr para aplicação como biomaterial.*** 2001, 140p. Tese (Doutorado em Tecnologia Nuclear – Materiais) – Instituto de Pesquisas Energéticas e Nucleares, IPEN/CNEN-SP, São Paulo.

9 Yu, S.Y.; Brodrick, C.W.; Ryan, M.P.; Scully, J.R. Effects of Nb and Zr alloying additions on the activation behavior of Ti in hydrochloric acid. ***Journal of the Electrochemical Society***, v.146, n.12, p.4429-4438,1999.

10. Pan, J.; Thierry, D.; Leygraf, C. Electrochemical impedance spectroscopy study of the passive oxide film on titanium for implant application. ***Electrochimica Acta.***; v.41, n.7/8, p.1143-1153, 1996.

11. Pan, J.; Thierry, D.; Leygraf, C. Hydrogen peroxide toward enhanced oxide growth on titanium in PBS solution: Blue coloration and clinical relevance. ***Journal of Biomedical Materials Research***. v.30, p.393-402,1996.

12. Pan, J.; Liao, H.; Leygraf, C.; Thierry, D.; Li; J. Variation of oxide films on titanium induced by osteoblast-like cell culture and the influence of an H_2O_2 pretreatment. ***Journal of Biomedical Materials Research***. v.40, p.244-256,1998.

13. Palomino, L.E.M. ***Caracterização microestrutural e estudo por espectroscopia de impedância eletroquimica da resistência à corrosão da liga de alumínio 2024-T3, utilizada na industria aeronautica, revestida com camada de conversão ambientalmente amigável.*** 2004, 198p. Dissertação, Universidade de São Paulo - USP, São Paulo.